![NRAP - National Risk Assessment Partnership]

Assessing the Impact of CO_2 Leakage in a Groundwater Aquifer in the Presence of Conceptual and Parametric Uncertainties

21 April 2017

Disclaimer

This report was prepared as an account of work sponsored by an agency of the United States Government. Neither the United States Government nor any agency thereof, nor any of their employees, makes any warranty, express or implied, or assumes any legal liability or responsibility for the accuracy, completeness, or usefulness of any information, apparatus, product, or process disclosed, or represents that its use would not infringe privately owned rights. Reference therein to any specific commercial product, process, or service by trade name, trademark, manufacturer, or otherwise does not necessarily constitute or imply its endorsement, recommendation, or favoring by the United States Government or any agency thereof. The views and opinions of authors expressed therein do not necessarily state or reflect those of the United States Government or any agency thereof.

This report (LLNL-TR-654900) has been reviewed by Lawrence Livermore National Laboratory and approved for public release.

Cover Illustration: Uncertainty quantification protocol.

An electronic version of this report can be found at:
http://www.netl.doe.gov/research/on-site-research/publications/featured-technical-reports

https://edx.netl.doe.gov/nrap

Assessing the Impact of CO₂ Leakage in a Groundwater Aquifer in the Presence of Conceptual and Parametric Uncertainties

K. Mansoor, Y. Sun, W. J. Trainor-Guitton, S. A. Carroll

Lawrence Livermore National Laboratory, 7000 East Avenue, Livermore, CA 94551

This page intentionally left blank.

Table of Contents

List of Figures

List of Tables

Acronyms, Abbreviations, and Symbols

Term	Description
3-D	Three-dimensional
CO_2	Carbon dioxide
KGS	Kansas Geological Survey
KLE	Karhunen-Loeve expansion
LLNL	Lawrence Livermore National Laboratory
NETL	National Energy Technology Laboratory
NRAP	National Risk Assessment Partnership
NUFT	Non-Isothermal, Unsaturated and Saturated Flow and Transport
ROM	Reduced-order model
TDS	Total dissolved solids
UQ	Uncertainty quantification
USDA	United States Department of Agriculture
WWC5	Water Well Completion Record

Acknowledgments

ABSTRACT

This study provides a science-based methodology to quantify impacts of carbon dioxide (CO$_2$) leakage from deep underground storage sources, transmitted along a wellbore into a shallow groundwater aquifer. This risk-based quantification was based on simulating coupled physical and chemical processes to predict how the natural system behaves over time in which the inherent uncertainty was propagated throughout the predictive process. Process model results were used to produce reduced-order models (ROMs), which represent the state of a system without the rigors of a complex and computationally intensive model. Among many uncertain input parameters, uncertain geological structure, rock properties (permeability, porosity, capillary-pressure parameters, etc.), and CO$_2$ and brine leakage rates over time were considered. The High Plains Aquifer was used in this study to represent a typical sedimentary aquifer that might overlay a CO$_2$ storage reservoir. Aquifer heterogeneity was characterized by deriving correlation lengths for geologic units identified from well logs in the High Plains Aquifer. The resulting ROMs describe plume characteristics that exceed specific water quality thresholds. Impact profiles developed from the ROMs encompass a larger global state of the system as a consequence of the increased parameter sampling density.

1. __INTRODUCTION__

Increasing anthropogenic contributions of carbon dioxide (CO_2) is considered to be a primary contributor to global climate change which will lead to repercussions to human and ecological health and well-being (Haines et al., 2006; McCarty, 2001; McMichael et al., 2006; Walther et al., 2002). Deep underground storage of CO_2 from stationary sources such as power plants and industrial processes is a promising strategy that may partially mitigate the effects of global climate change (IEA, 2008; IPCC, 2005; NETL, 2010). However, long-term storage of CO_2 in deep underground reservoirs requires a careful assessment of the reservoir integrity, well and fault susceptibility as leakage pathways, and impact of leaks on shallow groundwater resources and the atmosphere (Bachu, 2008; Benson, 2007; Herzog et al., 2003). Leakage into groundwater resources may adversely affect water quality by increasing the total dissolved solids (TDS) or by depressing the pH and dissolving naturally occurring trace metals from minerals (Carroll et al., 2009; Keating et al., 2011; Lu et al., 2010; Apps et al., 2010; Wang and Jaffe, 2004). In principle, the full range of groundwater impacts can be assessed though rigorous iterative numerical modeling; however, accurate predictions are complicated by data and parametric uncertainties needed to describe leakage sources and the chemical and physical properties of the aquifer system.

One hurdle for accurate process simulations is the spatial randomness of geological systems. One popular method to describe spatial randomness of geological systems is the Karhunen-Loeve expansion (KLE), which simultaneously solves stochastic partial differential equations for flow and transport (Karhunen, 1947; Zhang and Lu, 2004; Li and Zhang, 2007; Chen et al., 2013). Due to the difficulty and computational expense of solving stochastic partial differential equations of flow and transport, the KLE method has not been used extensively. As an alternative, a geological system can mathematically characterize the geologic system prior to solving flow and transport equations by a canonical representation of the transition-probability matrix (Carle and Fogg, 1996, 1997; Dai et al., 2007). Estimations of both lithologic heterogeneity and parametric uncertainties in geological units are needed to assess the impact that CO_2 and brine leakage will have on groundwater quality, although these calculations are currently computationally intensive.

Recently, uncertainty quantification methods have been used to characterize and quantify uncertainties of complex models of CO_2 sequestration involving multi-phase and multi-component reactive transport (Lu et al., 2012; Refsgaard et al., 2012; Sun et al., 2012a,b, 2013; Zhang and Sahinidis, 2012; Keating et al., 2011; Liu and Zhang, 2011; Oladyshkin et al., 2011; Tartakovsky et al., 2011). These approaches are considered to be intrusive and non-intrusive (Chen et al., 2013). Intrusive methods require a heavy mathematical manipulation and modification in existing simulation codes and can provide rigorous and accurate prediction of output uncertainties. Non-intrusive (sampling-based polynomial chaos expansion) methods have been widely used for their effectiveness and simplicity in solving practical problems. Using a non-intrusive method, uncertainties are introduced through input parameters to a selected simulation model in the form of probability distributions. Sample points generated from parameter probability distributions are propagated through the deterministic simulations. The simulated outputs are used to train the input-output relationships and to compute model statistics as reduced-order models

(ROMs) or emulations (Chen et al., 2013). Conceptually, this framework, as shown in Figure 1, is an iterative process whereby each new generation could have a reduced parameter set, define narrower bounds on the parameter distributions, and or increased complexity resulting in greater confidence in the risk profiles. In theory, the polynomial-based higher order models should be able to emulate the outcome of the numerical model but with less complexity and significantly faster simulation times to generate risk-based profiles.
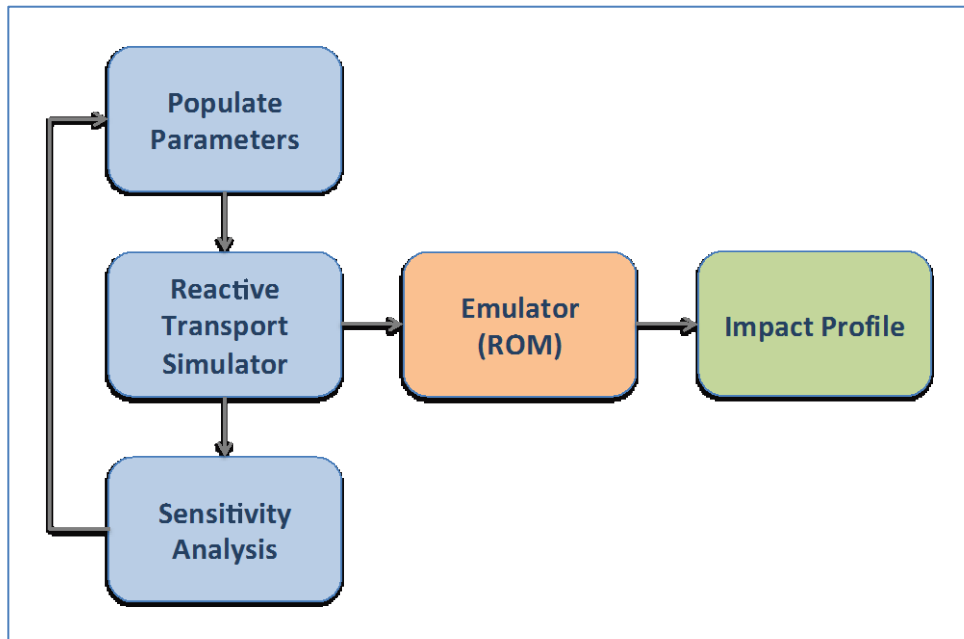
Figure 1: Uncertainty quantification protocol.

This report presents a framework to compute impacts of CO_2 and brine leakage from a storage reservoir on shallow groundwater chemistry by using non-intrusive sampling-based uncertainty quantification. Central to this approach is the development of three-dimensional (3-D) transitional probability-based lithologic models that are conditioned to well-log data, variations in numerous model parameters, and high-fidelity physics model of multi-phase multi-component reactive transport simulations. The simulated results are used to assess parameter sensitivity and to develop high-fidelity ROMs that describe groundwater impacts in terms of change in pH and TDS.

2. __METHODOLOGY__

This section describes the science-based methodology used to quantify impacts of CO_2 and brine leakage into a shallow groundwater aquifer from a single leaking well. The process involved using an uncertainty quantification code to generate 1,000 reactive-transport models that were sampled over defined parameter ranges to simulate physical and chemical processes, to conduct a sensitivity analysis of all varied parameters, and to build ROMs that provided statistical approximations of specific output that capture the uncertainty and allow impact to groundwater chemistry to be assessed.

This study mainly focused on the uncertainties of geological architecture, rock properties, and the leakage source term. Uncertain parameters and their ranges are listed in Table 1. Porosity, density, permeability and van Genuchten unsaturated parameters were taken from the United States Department of Agriculture (USDA) Rosetta database (Schaap et al., 2001). The leakage CO_2 and brine leakage fluxes (Figure 2) were estimated from deterministic simulations of leakage through a single wellbore of variable permeability and distance from the injection well corresponding to 50 years of CO_2 injection into the reservoir and 50 years of post-injection.
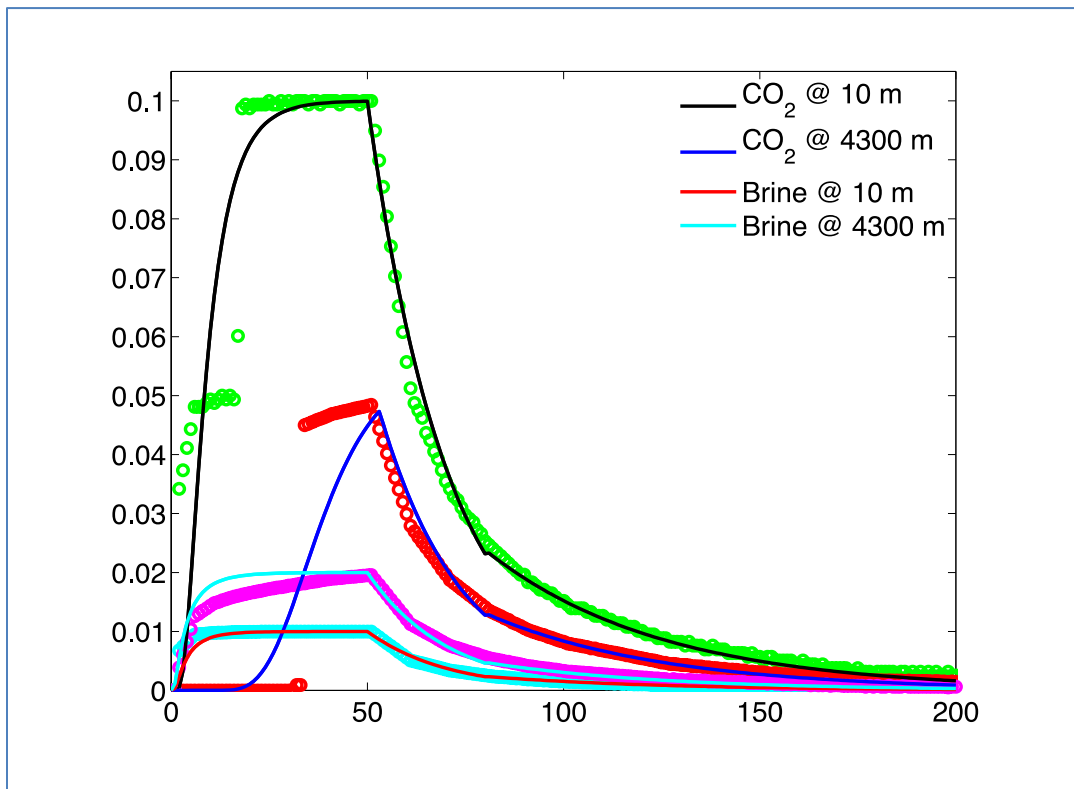

Figure 2: Simulated (symbols) and fitted (solid line) CO_2 and brine wellbore leakage rates. The green and the blue symbols correspond to the simulated CO_2 leakage rate at 10 and 4,300 m distance from the injection well, respectively. The red and the cyan symbols represent simulated brine leakage rate at 10 and 4,300 m respectively.

Table 1: Model parameters and input ranges. Some parameters were reduced to a median value based on screening simulations, which showed no sensitivity to the output fluxes. Screen ranges are shown here for reference.

x	Parameter	Screening Model	Refined Model
x_1	Sand-volume fraction	0.35 ~ 0.65	0.35 ~ 0.65
x_2	Correlation length in x-direction (m)	200 ~ 2,500	200 ~ 2,500
x_3	Correlation length in y-direction (m)	200 ~ 2,500	1,350
x_4	Correlation length in z-direction (m)	0.50 ~ 25.00	0.50 ~ 25.00
x_5	Sand porosity	0.25 ~ 0.50	0.38
x_6	Clay porosity	0.33 ~ 0.60	0.47
x_7	van Genuchten m in sand	0.52 ~ 0.79	0.66
x_8	van Genuchten m in clay	0.06 ~ 0.32	0.19
x_9	van Genuchten α in sand ($\log_{10} Pa^{-1}$)	-4.69 ~ -3.81	-4.69 ~ -3.81
x_{10}	van Genuchten α in clay ($\log_{10} Pa^{-1}$)	-5.50 ~ -4.14	-4.82
x_{11}	Permeability in sand ($\log_{10} m^2$)	-12 ~ -9	-12 ~ -9
x_{12}	Permeability in clay ($\log_{10} m^2$)	-18 ~ -15	-18 ~ -15
x_{13}	CO_2 diffusivity ($\log_{10} m^2 s^{-1}$)	-10 ~ -8	-9
x_{14}	CO_2 leakage flux scaling parameter	0 ~ 1.0	0 ~ 1.0
x_{15}	Brine leakage flux scaling parameter	0 ~ 1.0	0 ~ 1.0
x_{16}	Brine concentration ($Na^+ + Cl^-$ mol kg^{-1})	0.6 ~ 6.0	0.6 ~ 6.0
x_{17}	Time (years)	0–100	0–100

2.1 LITHOLOGIC MODEL

The High Plains Aquifer was used in this study to represent a typical sedimentary aquifer that might overlay a CO_2 storage reservoir (Figure 3). The aquifer, also known as the Ogallala Aquifer, is one of the largest aquifers in the world covering about 450,000 km^2 and spans eight states in the Great Plains. The aquifer accounts for approximately 27% of all irrigated land in the United States and about 30% of all groundwater used for irrigation (USGS, 2011). It is comprised mainly of unconsolidated or partly consolidated deposits of silt, sand, gravel and clay rock debris deposited 2~6 million years ago in the late Miocene to early Pliocene period when the Rocky Mountains were tectonically active. The underlying bedrock units range in age from Permian to Quaternary and consists of siltstone, shale, loosely to moderately cemented clay and silt, chalk, limestone, dolomite, conglomerate, claystone, gypsum, anhydrite, and bedded salt (Gutentag et al., 1984).
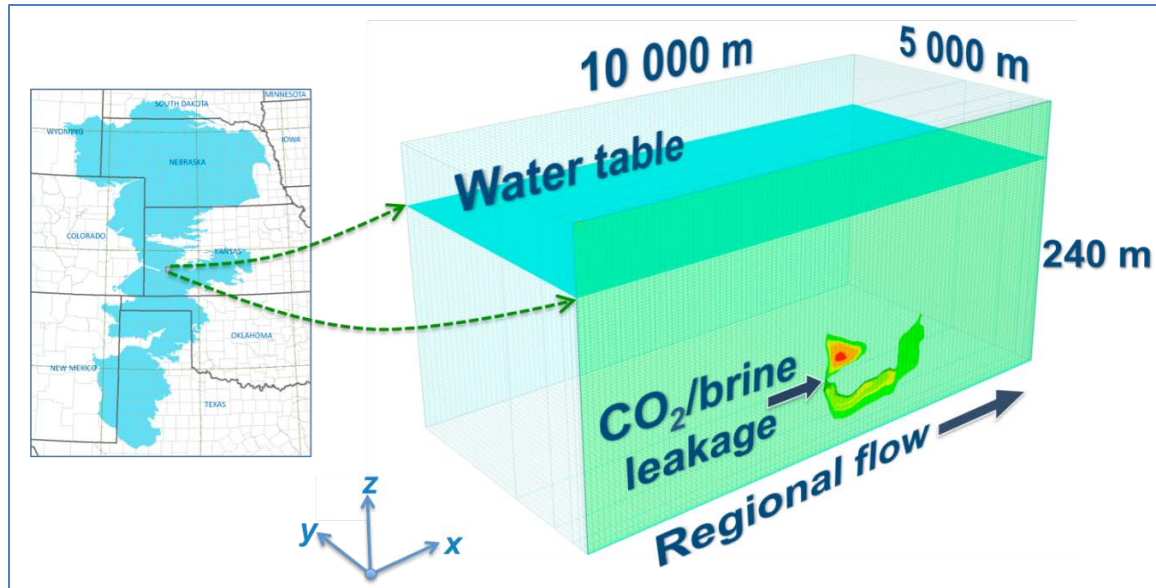
Figure 3: Site location and conceptual model.

The top 300 m of the aquifer was used to develop a lithological model for the geological realizations of the numerical model. Lithologic descriptions were obtained from the Kansas Geological Survey, Water Well Completion Record (WWC5) database (KGS, 2011). Approximately 100,000 picks from 11,454 wells were used to create a regional (162 km × 142 km) 3-D lithological model. All simulations were based on a smaller 10 km × 5 km portion of the lithological model to represent the extent of the numerical model. This smaller domain lies primarily in Haskel County, Kansas and was selected due to the relative higher density of lithological picks located at a depth sufficient enough to represent the model depth of 240 m. A total of 48 wells lie within this sub-domain. The wells are a mix of domestic, feedlot, irrigation, public water supply and oil field water supply wells which make up 468 lithological picks.

Aquifer heterogeneity was characterized by deriving spatial correlation lengths from the observed lithology proportion and distribution. The lithology was initially reclassified into six categories representing the primary well log descriptions and sorted into groups with similar permeability characteristics, then subsequently separated into two category classification to represent high and low permeability zones. The two-category classification was used to develop geostatistically derived indicator models using the TPROGS software (Carle, 1999). The main processes involve: (1) calculation of transition probability measurements, (2) modeling spatial variability using Markov chains, and (3) generation of an indicator-based conditioned random field. Traditional geostatistics involves fitting a mathematical function based on a spatial distribution of a property and implementing an estimation or simulation procedure to define property values for an entire domain. The transition probability approach estimates the likelihood of a particular property based at a lag distance instead of applying a traditional variogram model as the measure of spatial variability. This method also considers all other cross-correlational information. For this study area, the high permeability volume fraction was assigned a range 0.35 to 0.65 based on record distributions. The correlation lengths were

derived from the transition probability approach by using the ranges which transitions from high to low permeability materials were expected to occur along the primary x, y and z-directions. The correlation lengths in the x-direction and y-direction varied uniformly from 200~2,500 m and the correlation length in z-direction varied uniformly from 0.50~25.0 m. A total of 1,000 conditional geostatistical realizations were generated based on randomly selected material-volume fraction and correlation lengths populated using the PSUADE uncertainty quantification code (Tong, 2005, 2010).

2.2   REACTIVE TRANSPORT MODEL

The NUFT (Non-Isothermal, Unsaturated and Saturated Flow and Transport) code (Nitao, 1998; Hao et al., 2010) is employed as the primary simulator for the flow and reactive transport model to simulate the geochemical processes driven by CO₂ and brine leakage through an abandoned well from a CO₂ storage reservoir. NUFT is a highly flexible non-isothermal, multiphase flow and transport model based on the finite volume method which has been extensively verified and used for a variety of subsurface flow and transport problems including nuclear waste disposal, groundwater remediation, CO₂ sequestration and hydrocarbon production. Reactive transport was solved in the unsaturated and saturated zones assuming full multiphase flow including water-CO₂ partitioning between the gas and liquid phases. A limited amount of chemistry was included to account for changes in groundwater pH due to CO₂ dissolution as well as dissolved sodium and chloride as indicators of TDS. The dissolution of CO₂ in groundwater promotes the following sets of reactions:

$$CO_2(g) \leftrightarrow CO_2(aq) \tag{1}$$

$$CO_2(aq) + H_2O \leftrightarrow HCO_3^- + H^+ \tag{2}$$

$$CaCO_3(calcite) + H^+ \leftrightarrow Ca^{2+} + HCO_3^- \tag{3}$$
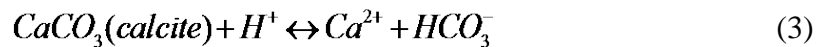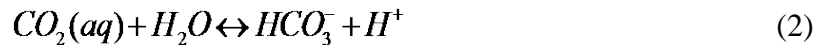
These reactions promote the acidification of the system which is then buffered by calcite dissolution. An isothermal condition is assumed with a generic temperature of 17°C in the entire domain because temperature variations over a 240-m aquifer depth are limited.

The numerical model domain was comprised of a 3-D bi-modally distributed heterogeneous domain representing the unsaturated and saturated zones of the High Plains Aquifer (Section 2.1 Lithologic Model). The model domain extends to 10,000 m × 5,000 m × 240 m (Figure 3) with a single leakage source placed at a depth of 198 m on the southern face. The east (minimum x) and west (maximum x) model boundaries are fixed in time, and the hydrostatic pressure gradient is imposed by changing the direction of the gravity vector. Since the regional groundwater flow of the Great Plains Aquifer in southwestern Kansas flows eastward, the mesh was structured to accommodate flow in the predominant x-direction maintained by a 0.3% hydraulic gradient. The southern (minimum y), northern (maximum y) and bottom (minimum z) boundaries are assumed to

be no-flow. A constant-pressure boundary condition is set on ground surface and at the aquifer bottom to maintain a hydrostatic initial condition with saturated and unsaturated zones.

The grid dimensions of the numerical model are n_x=101, n_y =11, n_z =101 for a total of 112,211 nodes. The numerical grid is orthogonally-based with fixed cell widths in the x (Δx=100.0 m) and Z (Δz =2.3762 m) directions with a telescoping variable width mesh in the y-direction (Δy={2, 3, 5, 10, 20, 50, 110, 200, 500, 1,100, 3,000} m). A telescoping mesh was used for numerical and computational efficiency. Due to differences in the lithologic and model meshgrids, a mesh-mapping procedure was implemented whereby a model cell is assigned by the greatest volume of lithologic cells occupying a single cell. Each simulation was executed for 20–40 hours each using the high performance computing clusters at Lawrence Livermore National Laboratory (LLNL). Parallelization of the simulations and subsequent analysis was required; otherwise this work would not be achievable.

2.3   UNCERTAINTY QUANTIFICATION

The PSUADE code was developed for uncertainty quantification (UQ) tasks such as forward uncertainty propagation, qualitative and quantitative sensitivity analysis, parameter exploration, risk analysis, and numerical optimization (Tong, 2005, 2010). It employs the non-intrusive or sampling-based approach to UQ that does not require simulation codes to be modified and ensures that it can easily be integrated with a variety of application simulators. PSUADE is equipped with many response-surface generation and validation techniques. These techniques can be coupled with other UQ techniques such as numerical optimization and Markov Chain-Monte Carlo methods for calibration and parameter estimation.

PSUADE was used to establish sampling points for the reactive transport simulations, to conduct parameter sensitivity analysis, and develop a ROM for the simulated results. Latin hypercube (McKay et al., 1979) sampling method was used to generate parameter values for the groundwater models, a Sobol sensitivity analysis of the successful runs to test the overall model response to individual parameters for each time step, and the LP-tau (Shukhman, 1994) quasi random sequence generator to produce 200,000 sample points using the ROM to produce the necessary statistical output for uncertainty quantification.

ROMs offer a cost-effective representation of a full-scale system. These emulations represent objective functions captured by full physics simulations by considering the same inputs (x) and response variable (y) as presented in a higher order polynomial:

$$y=a_0+ \sum_i a_i x_i+ \sum_i \sum_j a_{ij} x_i x_j + \sum_i \sum_j \sum_k a_{ijk} x_i x_j x_k+\ldots \qquad (4)$$

where *a* represents the polynomial fitting coefficients and *i*, *j* and *k* are indices of the uncertain parameters defined in Table 1. This reduced analytical form permits a greater magnitude of model simulations that more uniformly sample parameter variability to

better represent the system uncertainty. The execution time for a ROM with 200,000
emulations takes only a few minutes.

This study developed emulations that mark the extent of pH and TDS plume length, area,
and volumes at specific thresholds over the parameter space defined in Table 1. The time
variable was incorporated into the emulations to represent the process dynamically. This
significantly improved model usability and data management. In addition, input
parameters were normalized from 0–1 to avoid ill-conditioning, whereby parameters with
the largest magnitudes could greatly skew the emulation results due to the carry over of
floating point errors.

3. <u>RESULTS AND DISCUSSION</u>

This section evaluates the overall sensitivity of the variable parameters to pH and TDS output and the fidelity of the emulations to match the simulated results.

3.1 PARAMETER SENSITIVITY

Sobol's global sensitivity analysis (Sobol, 1993, 2001) on the simulation output estimates the contribution each input parameter had on the variance of the output. Tables 2 and 3 summarize the screening model and refined model, respectively. The refined model used median values for six parameters in the refined model because they were insensitive to the flux outputs in the screening analysis. The sensitivity results were used to reduce the number of variable parameters from 16 to 10 between screening and refined models (brine leakage was not considered in the screening model). Values for correlation length in y, sand and clay porosity, sand and clay van Genuchten m and CO$_2$ diffusivity have an insignificant impact on the model output and were fixed at their mean values for the refined model (Table 1).

For the refined model, sand permeability and CO$_2$ leakage rate were evaluated to have the greatest impact on the pH plume sizes; and sand permeability, brine leakage and brine concentration were assessed to have the greatest impact on the TDS plume sizes based on their global Sobol indices summarized in Table 3.

A second observation is that screening model leakage rates, sand permeability, and clay permeability show different time-dependent trends for area and volume outputs. Variability of CO$_2$ and brine leakage rates had the greatest impact on pH and TDS plume size, becoming increasingly more sensitive up to the end of injection, at which point the sensitivity of this parameter leveled off. Whereas the sensitivity to variation in sand permeability consistently increased at each time interval and the sensitivity to variations in clay permeability displayed the reverse trend with time.

Table 2: Summary of correlation coefficients (R^2) and normalized Sobol sensitivity indices for the screening model, at pH < 6.5. x01 to x14 refer to the model parameters

Output	Time (y)	R^2	x01	x02	x03	x04	x05	x06	x07	x08	x09	x10	x11	x12	x13	x14
Plume distance	10	0.851	0.022	0.014	0.016	0.035	0.046	0.014	0.019	0.031	0.020	0.027	0.764	0.077	0.021	0.011
	30	0.966	0.006	0.014	0.009	0.007	0.035	0.009	0.009	0.022	0.015	0.013	0.871	0.024	0.019	0.019
	50	0.982	0.005	0.025	0.012	0.009	0.025	0.014	0.015	0.024	0.018	0.014	0.834	0.033	0.020	0.030
	80	0.978	0.005	0.023	0.012	0.011	0.029	0.017	0.016	0.018	0.023	0.018	0.833	0.040	0.021	0.025
	100	0.960	0.006	0.020	0.014	0.013	0.035	0.014	0.015	0.019	0.025	0.021	0.838	0.042	0.021	0.029
	global	0.961	0.061	0.062	0.058	0.059	0.066	0.049	0.078	0.076	0.069	0.064	0.567	0.066	0.064	0.072
pH plume area in X~Y plane	10	0.911	0.154	0.056	0.047	0.095	0.090	0.027	0.042	0.156	0.104	0.023	0.134	0.290	0.041	0.170
	30	0.970	0.101	0.073	0.049	0.062	0.074	0.026	0.046	0.127	0.085	0.043	0.102	0.292	0.058	0.243
	50	0.971	0.075	0.056	0.065	0.063	0.074	0.032	0.042	0.078	0.079	0.058	0.163	0.228	0.046	0.276
	80	0.944	0.041	0.083	0.037	0.041	0.079	0.021	0.039	0.069	0.042	0.089	0.197	0.241	0.068	0.319
	100	0.966	0.044	0.046	0.036	0.036	0.057	0.023	0.037	0.052	0.038	0.084	0.319	0.197	0.034	0.315
	global	0.963	0.163	0.122	0.129	0.094	0.100	0.131	0.165	0.175	0.141	0.105	0.181	0.184	0.112	0.190
pH plume volume	10	0.905	0.084	0.059	0.053	0.108	0.136	0.048	0.067	0.118	0.096	0.065	0.097	0.317	0.060	0.137
	30	0.964	0.053	0.070	0.037	0.074	0.124	0.041	0.067	0.083	0.074	0.072	0.106	0.267	0.062	0.255
	50	0.948	0.047	0.041	0.053	0.060	0.116	0.058	0.051	0.044	0.062	0.051	0.191	0.171	0.048	0.299
	80	0.880	0.020	0.080	0.043	0.064	0.137	0.038	0.043	0.074	0.032	0.047	0.285	0.149	0.074	0.300
	100	0.960	0.013	0.029	0.013	0.022	0.079	0.032	0.027	0.019	0.012	0.027	0.507	0.086	0.019	0.328
	global	0.947	0.112	0.118	0.104	0.096	0.117	0.131	0.155	0.132	0.126	0.101	0.214	0.140	0.106	0.187

Table 3: Summary of correlation coefficients (R^2) and normalized Sobol sensitivity indices for the refined model. x01 to x16 refer to the model parameters

| Threshold	Output	R^2	x01	x02	x04	x09	x11	x12	x14	x15	x16
ph < 5.5	Plume distance	0.864	0.042	0.055	0.064	0.050	0.115	0.081	0.275	0.048	0.062
	Plume area in X~Y plane	0.942	0.033	0.038	0.040	0.038	0.322	0.093	0.384	0.018	0.025
	Plume volume	0.969	0.023	0.013	0.010	0.020	0.355	0.024	0.433	0.015	0.013
ph < 6.0	Plume distance	0.886	0.068	0.087	0.061	0.046	0.396	0.076	0.127	0.042	0.043
	Plume area in X~Y plane	0.962	0.018	0.025	0.020	0.025	0.213	0.082	0.407	0.011	0.014
	Plume volume	0.983	0.008	0.006	0.005	0.003	0.178	0.009	0.465	0.003	0.004
ph < 6.5	Plume distance	0.929	0.080	0.041	0.029	0.024	0.609	0.049	0.066	0.019	0.027
	Plume area in X~Y plane	0.958	0.013	0.036	0.022	0.017	0.091	0.067	0.429	0.013	0.015
	Plume volume	0.978	0.006	0.004	0.005	0.004	0.049	0.009	0.480	0.003	0.003
ph < 7.0	Plume distance	0.949	0.056	0.033	0.014	0.014	0.673	0.022	0.038	0.009	0.015
	Plume area in X~Y plane	0.941	0.026	0.040	0.040	0.021	0.088	0.062	0.402	0.020	0.015
	Plume volume	0.955	0.018	0.010	0.013	0.009	0.128	0.015	0.420	0.008	0.008
ph < 7.5	Plume distance	0.957	0.040	0.023	0.012	0.009	0.700	0.021	0.029	0.008	0.013
	Plume area in X~Y plane	0.878	0.044	0.027	0.053	0.032	0.432	0.058	0.237	0.027	0.030
	Plume volume	0.864	0.025	0.035	0.025	0.028	0.470	0.049	0.264	0.028	0.033
TDS > 1,000 mg L^{-1}	Plume distance	0.905	0.060	0.074	0.039	0.037	0.587	0.065	0.027	0.227	0.156
	Plume area in X~Y plane	0.899	0.049	0.065	0.082	0.033	0.318	0.040	0.050	0.329	0.255
	Plume volume	0.914	0.053	0.029	0.046	0.041	0.269	0.053	0.037	0.401	0.263
TDS > 1,500 mg L^{-1}	Plume distance	0.891	0.060	0.099	0.067	0.056	0.490	0.063	0.041	0.290	0.223
	Plume area in X~Y plane	0.897	0.062	0.063	0.079	0.036	0.268	0.058	0.049	0.369	0.254
	Plume volume	0.922	0.075	0.024	0.039	0.033	0.265	0.042	0.035	0.417	0.253
TDS > 5,000 mg L^{-1}	Plume distance	0.908	0.105	0.077	0.056	0.066	0.408	0.055	0.047	0.409	0.216
	Plume area in X~Y plane	0.912	0.058	0.060	0.057	0.043	0.275	0.055	0.062	0.435	0.221
	Plume volume	0.952	0.075	0.030	0.040	0.041	0.368	0.039	0.029	0.348	0.259

3.2   MODEL PERFORMANCE

A total of 1,000 reactive-transport simulations were attempted for each wellbore model iteration, of which, 590 and 714 simulations executed successfully for the 100-year simulation period for the screening model and the refined model, respectively. Failure of simulations to converge within the allotted 40 hours was generally due to large pressure build-ups in the low permeability zones in the vicinity of the source zone. Threshold specific pH and TDS ROMs were generated to provide statistical approximation of the maximum length, X~Y area, and volume of the impacted aquifer from the completed reactive transport simulations.

Figure 4 shows the number of simulations for a specific threshold as a function of time. Generally ROMs derived from less than 600 successful simulations yielded higher fidelity ROMs. For this reason, ROMs underperform at times less than 30 years and pH below 5.50 and TDS above 2,000 ppm. In general, smaller numbers of simulations are produced at the lower pH and higher TDS thresholds. This is important when establishing threshold limits for ROMs since the fidelity of the ROMs decreases with a reduction of successful simulations.

The goodness of fit between simulated and emulated results for aquifer plume area, and volume impacted by CO$_2$ and brine for the refined model is summarized in the R^2 column on Table 3 and shown graphically in Figure 5 for plume volumes and areas for thresholds pH $\geq$ 6.5 and TDS $\leq$ 1,500 mg/L. The overall performance of the ROM was assessed by its ability to reproduce output from the reactive-transport simulation using the coefficient of determination:

$$R^2 = \frac{\sum_i \left(\hat{y}_i - \bar{y}\right)^2}{\sum_i \left(y_i - \bar{y}\right)^2} \tag{5}$$

where y_i is the simulated results, $\hat{y}_i$ is the emulated results and $\bar{y}$ is the mean of the simulated results. The pH plume volume, area, and length ROMs show good performance with R^2 varying between 0.86 and 0.98 for thresholds defined at pH 5.5, 6.0, 6.5, and 7.0. Performance of the TDS plume volume, area, and length ROMs was similar to that for the pH ROM with R^2 between 0.89 and 0.95 all thresholds. pH and TDS emulations slightly underestimated simulated plumes and result in a portion (11%) of non-physical negative results which were discarded in the groundwater impact analysis.
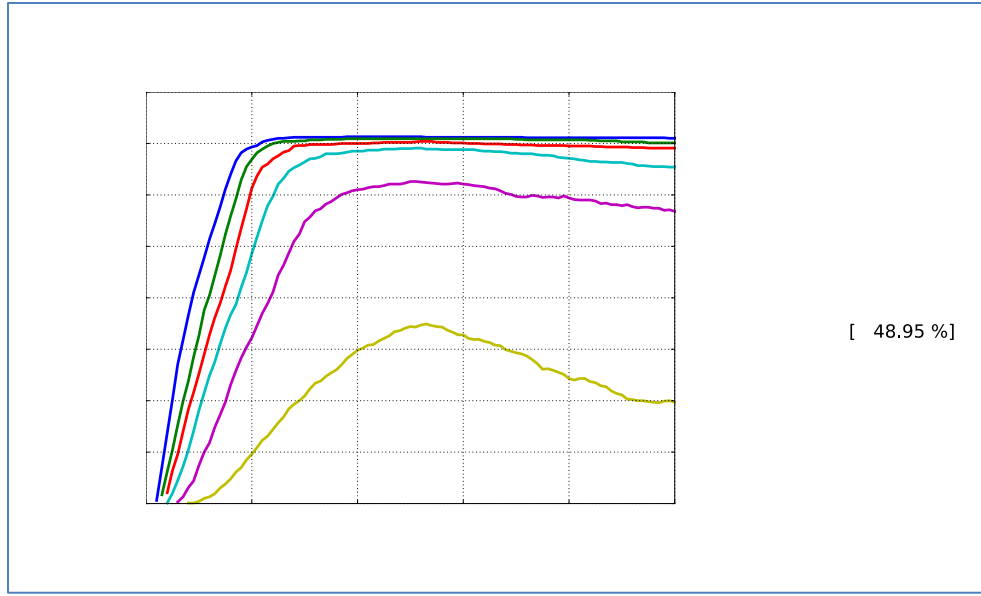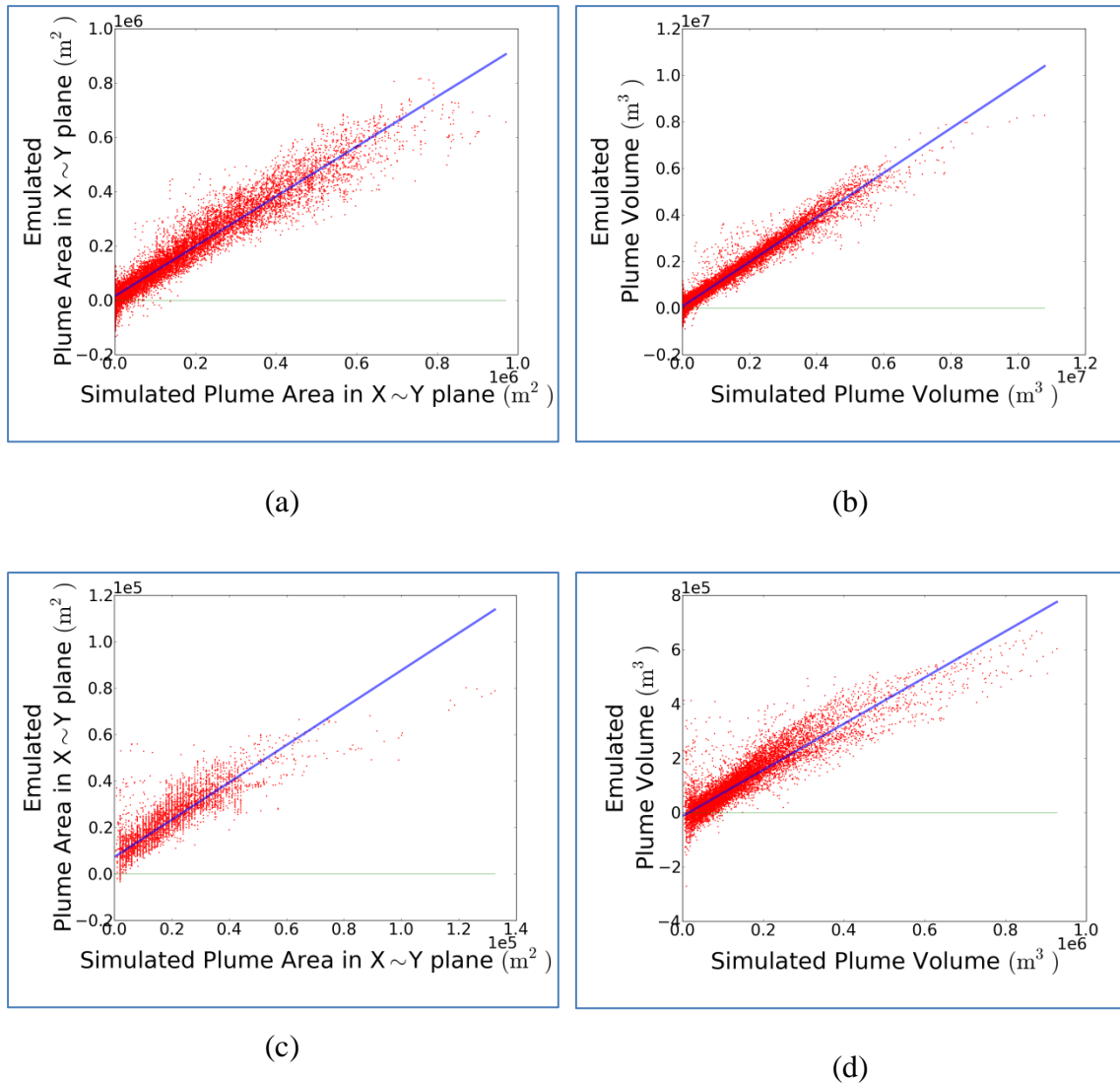
(a)
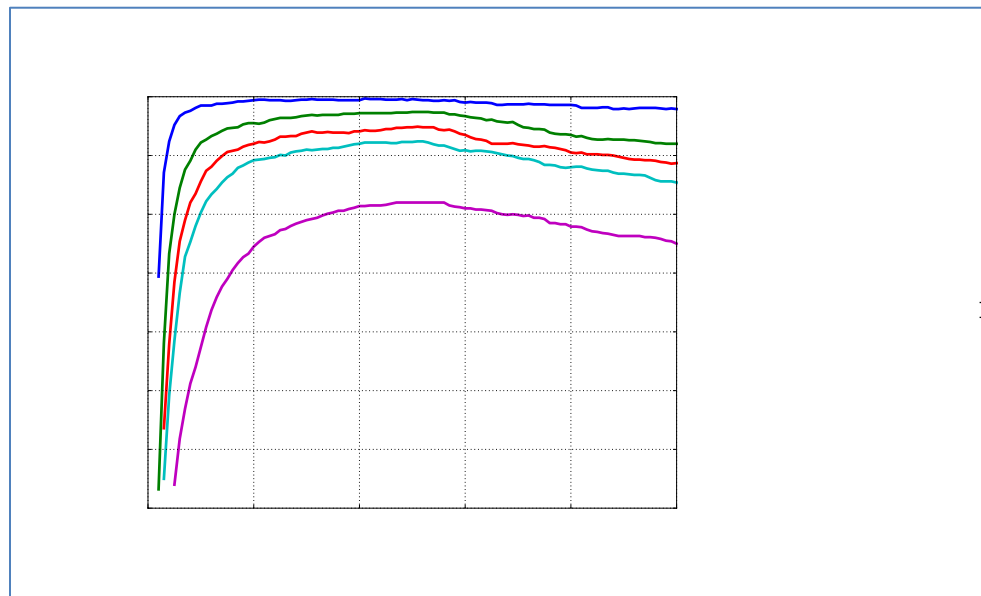
(b)

**Figure 4: (a) Simulation count vs. time for pH thresholds 7.5, 7.0, 6.5, 6.0, 5.5, and 5.25. (b)
Simulation count vs. time for TDS thresholds 500, 1,000, 1,500, 2,000, and 5,000 mg L⁻¹. Note:
Numbers within legend brackets refers to the percentage of successful simulations.**

(a)

(b)

(c)

(d)

Figure 5: Comparison of simulated and emulated (a) plume area in the X~Y plane for the refined model, pH < 6.5, (b) plume volume for the refined model, pH < 6.5, (c) plume area in the X~Y plane for the refined model, TDS > 1,500 mg L^{-1}, and (d) plume volume for the refined model, pH < 6.5, TDS > 1,500 mg L^{-1}.

ROM performance describe above points to a couple of trade-offs of using emulations to describe complex systems rather than continuum-based reactive transport simulations. The first trade-off is that the ROM introduces additional uncertainty in the outcome by virtue of its in-exact match to the simulated data. This limitation is offset by computation speed of the emulation that allows a more uniform and denser sampling to fully capture the uncertainty of the system. A second trade-off is that emulations described here are threshold and dimension (volume, area, length) specific whereas the simulations produce all output as a function of time and space. This requires prescribed thresholds to be

known prior to development of the ROM so that they will be most useful. This study is specific to a class of aquifers dominated by alternating layers of permeable sands and impermeable shales in response to a specific leakage scenario corresponding to 50 years injection and 50 years post-injection observations. In principle, site characterization data for similar class of aquifers to the High Plains Aquifer could be used to narrow the range of viable parameters and lower the overall uncertainty on the impact to the groundwater if CO$_2$ and brine were to leak. The ROMs developed here should not be used to assess leakage with different reservoir injection histories or for scenarios where leakage is mitigated.

4. **CONCLUSIONS**

This report presented a framework to compute impacts of CO_2 and brine leakage from a storage reservoir on shallow groundwater chemistry by using non-intrusive sampling-based uncertainty quantification. This approach made use of well log lithology, transitional probability, and parameter variability to account for aquifer heterogeneity; variation in time-dependent leakage source terms to account for CO_2 and brine flux into the aquifer for the storage reservoir; and multi-phase multi-component reactive transport simulations to develop high-fidelity ROMs that describe groundwater impacts in terms of change in pH and TDS. The ROMs were then used to fully sample conceptual and parameter variability and statistically assess impact to groundwater quality. Evaluation of the emulated results can provide valuable insight into the behavior of a potentially impacted aquifer over time and space and design of monitoring strategies.

The layered aquifer model chosen here investigated hypothetical leakage from a single wellbore into an aquifer with layered permeability with some calcite to buffer the pH. The results point to the need to reduce uncertainties in predicting the behavior of a natural system. This UQ based approach can be adapted to generalized aquifers for potential geologic carbon storage locations. A key finding of this study is that the most important parameters to constrain to reduce uncertainty are the CO_2 and brine leakage rates, brine concentration, sand permeability, and distance of the leaking well from the injection well. All other parameters appear to be secondary.

This page intentionally left blank.

5. REFERENCES

Apps, J. A.; Zheng, L.; Zhang, Z.; Xu, T.; Birkholzer, J. T. Evaluation of potential changes in groundwater quality in response to CO_2 leakage from deep geologic storage. *Transp. Porous Med.* **2010,** *82*, 215–246.

Bachu, S. CO_2 storage in geological media: Role, means, status, and barriers to deployment. *Prog. Energ. Combust.* **2008,** *34*, 254–273.

Benson, S. *Addressing long–term liability of carbon dioxide capture and geological sequestration*; Technical Report; World Resource Institute (WRI) Long–term liability Workshop, Washington, DC, June 7, 2007.

Carle, S. *T–PROGS: Transitional probability geostatistical software, Version 2.1 user manual*; University of California: Davis, CA, 1999.

Carle, S., Fogg, G. Modeling spatial variability with one– and multi–dimensional continuous markov chains. *Math. Geol.* **1997,** *29*, 891–918.

Carle, S.; Fogg, G. Transition probability–based indicator geostatistics. *Math. Geol.* **1996,** *28*, 453–476.

Carroll, S.; Hao, Y.; Aines, R. Geochemical detection of CO_2 in dilute aquifers. *Geochem. Trans.* **2009,** *10*, 4.

Chen, X.; Ng, B.; Sun, Y.; Tong, C. A flexible uncertainty quantification method for linearly coupled multi-physics systems. *J. Comput. Phys.* **2013,** *248*, 383–401.

Dai, Z.; Wolfsberg, A.; Lu, Z.; Ritzi, Jr., R. Representing aquifer architecture in macrodispersivity models with an analytical solution of the transition probability matrix. *Geophys. Res. Lett.* **2007,** *34*, L20406

Gutentag, E.; Heimes, F.; Krothe, N.; Luckey, R.; Weeks, J. *Geohydrology of the High Plains aquifer in parts of Colorado, Kansas, Nebraska, New Mexico, Oklahoma, South Dakota, Texas, and Wyoming*; Technical Report Professional Paper, 1400–B; U.S. Geological Survey, 1984.

Haines, A.; Kovats, R.; Campbell-Lendrum, D.; Corvalan, C. Climate change and human health: Impacts, vulnerability and public health. *U.S. Public Health* **2006,** *120*, 585–596.

Hao, Y.; Sun, Y.; Nitao, J. *Overview of NUFT â€" a versatile numerical model for simulating flow and reactive transport in porous media*; Bentham Science Publishers, 2010.

Herzog, H.; Caldeira, K.; Reilly, J. An issue of permanence: assessing the effectiveness of temporary carbon storage. *Clim. Change* **2003,** *59*, 293–310.

IEA. CO_2 Capture and storage: A key carbon abatement option; OECD Publishing, 2008; pp 264.

IPCC. IPCC special report on carbon dioxide capture and storage. Prepared by Working Group III of the Intergovernmental Panel on Climate Change. Metz, B., Davidson, O., de Coninck, H. C., Loos, M., Meyer, L. A., Eds.; Cambridge University Press:

Cambridge, United Kingdom and New York, NY; Technical Report; Intergovernmental Panel on Climate Change, 2005; pp 442.

Kansas Geological Survey (KGS). Wells, logs, core, and other databases. http://www.kgs.ku.edu/PRS/petroDB.html (accessed on Sept 2011).

Karhunen, K. Uber linare Methoden in der Wahrschein-Lichkeitsrechnung. *Ann. Acad. Sci. Fennicae. Ser. A. I. Math.-Phys.* **1947,** *37*, 1–79.

Keating, G.; Middleton, R.; Viswanathan, H.; Stauffer, P.; Pawar, R. How storage uncertainty will drive ccs infrastructure. *Energy Procedia* **2011,** *4*, 2393–2400.

Li, H.; Zhang, D. Probabilistic collocation method for flow in porous media. *Water Resour. Res.* **2007,** *43*.

Liu, B.; Zhang, Y. CO_2 modeling in a deep saline aquifer: a predictive uncertainty analysis using design of experiment. *Environ. Sci. Technol.* **2011,** *45*, 3504–3510.

Lu, C.; Sun, Y.; Buscheck, T.; Hao, Y.; White, J.; Chiaramonte, L. Uncertainty quantification of CO_2 leakage through a fault with multiphase and nonisothermal effects. *Greenhouse Gases: Sci. Technol.* **2012,** *2*, 445–459.

McCarty, J. Ecological consequences of recent climate change. *Conserv. Biol.* **2001,** *15*, 320–331.

McKay, M.; Beckman, R.; Conover, W. A comparison of three methods for selecting values of input variables in the analysis of output from a computer code. *Technometrics* **1979,** *21*, 239–245.

McMichael, A.; Woodruff, R.; Hales, S. Climate change and human health: present and future risks. *The Lancet* **2006,** *367*, 859–869.

NETL. *2010 Carbon sequestration atlas of the United States and Canada,* 3rd Edition; Technical Report; U.S. Department of Energy, Office of Fossil Energy, National Energy Technology Laboratory, 2010.

Nitao, J. J. *User's manual for the USNT module of the NUFT code, version 2 (NP-phase, NC-component, thermal)*; UCRL-MA-130653; Lawrence Livermore National Laboratory, Livermore, CA, 1998.

Oladyshkin, S.; Class, H.; Helmig, R.; Nowak, W. A concept for data-driven uncertainty quantification and its application to carbon dioxide storage in geological formations. *Adv. Water Resour.* **2011,** 1508–1518.

Refsgaard, J.; Christensen, S.; Sonnenborg, T.; Seifert, D.; HÃ¸jberg, A.; Troldborg, L.; Review of strategies for handling geological uncertainty in groundwater flow and transport modeling. *Adv. Water Resour.* **2012,** *36*, 36–50.

Schaap, M.; Leij, F.; van Genuchten, M. Rosetta: A computer program for estimating soil hydraulic parameters with hierarchical pedotransfer functions. *J. of Hydrol.* **2001,** *251*, 163–176.

Shukhman, B. Generation of quasi–random (lpÏ„) vectors for parallel computation. *Comp. Phys. Commun.* **1994,** *78*, 279–286.

Sobol, I. M. Global sensitivity indices for nonlinear mathematical models and their Monte Carlo estimates mathematics and computers in simulations. *Math. Comp. Simul* **2001,** 55, 271-280.

Sobol, I. M. Sensitivity analysis for nonlinear mathematical models, *Math. Model. Comput.* **1993,** 1, 407-414.

Sun, Y.; Buscheck, T.; Hao, Y. An analytical method for modeling first–order decay networks. *Comput. Geosci.* **2012a,** *39*, 86–97.

Sun, Y.; Tong, C.; Duan, Q.; Buscheck, T.; Blink, J. Combining simulation and emulation for calibrating sequentially reactive transport systems. *Transp. Porous Media* **2012b,** *92*, 509–526.

Sun, Y.; Tong, C.; Trainor-Guitton, W.; Lu, C.; Mansoor, K.; Carroll, S. Global sampling for integrating physics–specific subsystems and quantifying uncertainties of CO_2 geologic sequestration. *Intl. J. Greenhouse Gas Control* **2013,** *12*, 108–123.

Tartakovsky, D.; Nowak, W.; Bolster, D. Introduction to the special issue on uncertainty quantification and risk assessment. *Adv. Water Res.* **2011,** *36*, 1–2.

Tong, C. *PSUADE User's Manual*; LLNL-SM-407882; Lawrence Livermore National Laboratory, Livermore, CA, 2005.

Tong, C. Self–validated variance–based methods for sensitivity analysis of model outputs. *Reliab. Eng. Syst. Safe.* **2010,** *95*, 301–309.

U.S. Geological Survey (USGS), National water–quality assessment (nawqa) program: High plains regional ground water (hpgw) study. http://co.water.usgs.gov/nawqa/hpgw/HPGW_home.html (accessed on Sept 2011).

Walther, G. R.; Post, E.; Convey, P.; Menzel, A.; Parmesan, C.; Beebee, T.; Fromentin, J. M.; Hoegh-Guldberg, O.; Bairlein, F. Ecological responses to recent climate change. *Nature* **2002,** *416*, 389–395.

Wang, S.; Jaffe., P. Dissolution of mineral phase in potable aquifers due to CO_2 releases from deep formations, effect of dissolution kinetics. *Energy Convers. Manage.* **2004,** *45*, 2833–2848.

Zhang, D.; Lu, Z. An efficient, higher-order perturbation approach for flow in randomly heterogeneous porous media via Karhunen-Loeve decomposition. *J. Comput. Phys.* **2004,** *194*, 773–794

Zhang, Y.; Sahinidis, N. Uncertainty quantification in CO_2 sequestration using surrogate models from polynomial chaos expansion. *Ind. Eng. Chem. Res.* **2012**.

This page intentionally left blank.

NRAP is an initiative within DOE's Office of Fossil Energy and is led by the National Energy Technology Laboratory (NETL). It is a multi-national-lab effort that leverages broad technical capabilities across the DOE complex to develop an integrated science base that can be applied to risk assessment for long-term storage of carbon dioxide (CO_2). NRAP involves five DOE national laboratories: NETL, Lawrence Berkeley National Laboratory (LBNL), Lawrence Livermore National Laboratory (LLNL), Los Alamos National Laboratory (LANL), and Pacific Northwest National Laboratory (PNNL).

Technical Leadership Team

Diana Bacon
Lead, Groundwater Protection Working Group
Pacific Northwest National Laboratory
Richmond, WA

Jens Birkholzer
LBNL Lab Lead
Lawrence Berkeley National Laboratory
Berkeley, CA

Grant Bromhal
Technical Director, NRAP
Research and Innovation Center
National Energy Technology Laboratory
Morgantown, WV

Chris Brown
PNNL Lab Lead
Pacific Northwest National Laboratory
Richmond, WA

Susan Carroll
LLNL Lab Lead
Lawrence Livermore National Laboratory
Livermore, CA

Abdullah Cihan
Lead, Reservoir Performance Working Group
Lawrence Berkeley National Laboratory
Berkeley, CA

Tom Daley
Lead, Strategic Monitoring Working Group
Lawrence Berkeley National Laboratory
Berkeley, CA

Robert Dilmore
NETL Lab Lead
Research and Innovation Center
National Energy Technology Laboratory
Pittsburgh, PA

Nik Huerta
Lead, Migration Pathways Working Group
Research and Innovation Center
National Energy Technology Laboratory
Albany, OR

Rajesh Pawar
LANL Lab Lead
Lead, Systems/Risk Modeling Working Group
Los Alamos National Laboratory
Los Alamos, NM

Tom Richard
Deputy Technical Director, NRAP
The Pennsylvania State University
State College, PA

Josh White
Lead, Induced Seismicity Working Group
Lawrence Livermore National Laboratory
Livermore, CA

Sean Plasynski
Executive Director
Technology Development and
Integration Center
National Energy Technology Laboratory
U.S. Department of Energy

Heather Quedenfeld
Associate Director
Coal Development and Integration
National Energy Technology Laboratory
U.S. Department of Energy

Traci Rodosta
Technology Manager
Strategic Planning
Science and Technology Strategic Plans
and Programs
National Energy Technology Laboratory
U.S. Department of Energy

Darin Damiani
Program Manager
Carbon Storage
Office of Fossil Energy
U.S. Department of Energy

NRAP Executive Committee

Cynthia Powell
Executive Director
Research and Innovation Center
National Energy Technology Laboratory

Donald DePaolo
Associate Laboratory Director
Energy and Environmental Sciences
Lawrence Berkeley National Laboratory

Roger Aines
Chief Energy Technologist
Lawrence Livermore National
Laboratory

Melissa Fox
Program Manager
Applied Energy Programs
Los Alamos National Laboratory

George Guthrie
Chair, NRAP Executive Committee
Earth and Environmental Sciences
Los Alamos National Laboratory

Alain Bonneville
Laboratory Fellow
Pacific Northwest National Laboratory

Grant Bromhal
Technical Director, NRAP
Research and Innovation Center
National Energy Technology Laboratory

NRAP Technical Report Series